

## Formulation development and characterization of lumefantrine nanosuspension for enhanced antimalarial activity

Ripalkumar Shah, Tejal Soni, Unnati Shah, B. N. Suhagia, M. N. Patel, Tejas Patel, Gamal A. Gabr, Bapi Gorain & Prashant Kesharwani

To cite this article: Ripalkumar Shah, Tejal Soni, Unnati Shah, B. N. Suhagia, M. N. Patel, Tejas Patel, Gamal A. Gabr, Bapi Gorain & Prashant Kesharwani (2021) Formulation development and characterization of lumefantrine nanosuspension for enhanced antimalarial activity, Journal of Biomaterials Science, Polymer Edition, 32:7, 833-857, DOI: [10.1080/09205063.2020.1870378](https://doi.org/10.1080/09205063.2020.1870378)

To link to this article: <https://doi.org/10.1080/09205063.2020.1870378>



Published online: 15 Jan 2021.



Submit your article to this journal [↗](#)



Article views: 33




View related articles [↗](#)



View Crossmark data [↗](#)



## Formulation development and characterization of lumefantrine nanosuspension for enhanced antimalarial activity

Ripalkumar Shah<sup>a,b</sup>, Tejal Soni<sup>a</sup>, Unnati Shah<sup>b</sup>, B. N. Suhagia<sup>a</sup>, M. N. Patel<sup>a</sup>,  
Tejas Patel<sup>a</sup>, Gamal A. Gabr<sup>c,d</sup>, Bapi Gorain<sup>e,f</sup> and Prashant Kesharwani<sup>g</sup> 

<sup>a</sup>Faculty of Pharmacy, Dharamsinh Desai University, Nadiad, Gujarat, India; <sup>b</sup>Caplin Point Laboratories Limited (R&D), Chennai, Tamilnadu, India; <sup>c</sup>Department of Pharmacology and Toxicology, College of Pharmacy, Prince Sattam Bin Abdulaziz University, Al-Kharj, Saudi Arabia; <sup>d</sup>Agricultural Genetic Engineering Research Institute, Agriculture Research Center, Giza, Egypt; <sup>e</sup>School of Pharmacy, Faculty of Health and Medical Science, Taylor's University, Subang Jaya, Selangor, Malaysia; <sup>f</sup>Centre for Drug Delivery and Molecular Pharmacology, Faculty of Health and Medical Sciences, Taylor's University, Subang Jaya, Selangor, Malaysia; <sup>g</sup>Department of Pharmaceutics, School of Pharmaceutical Education and Research, New Delhi, Delhi, India

### ABSTRACT




Variable and low oral bioavailability (4–11%) of lumefantrine (LUF), an anti-malarial agent, is characterized by very low solubility in aqueous vehicle. Thus, the present study was intended to formulate lyophilized nanosuspensions of LUF to resolve its solubility issues for the improvement of oral bioavailability. A three level 3<sup>2</sup> factorial design was applied to analyze the influence of independent variables, concentration of polysorbate 80 (X<sub>1</sub>) and sonication time (X<sub>2</sub>) on the responses for dependent variables, particle size (Y<sub>1</sub>) and time to 90% release of LUF (t<sub>90</sub>) (Y<sub>2</sub>). Optimized formulation (F3) has shown to possess lowest particle size (95.34 nm) with minimum t<sub>90</sub> value (□ 3 mins), which was lyophilized to obtain the dry powder form of the nanosuspension. The characterization parameters confirmed the amorphous form of LUF with good stability and no chemical interactions of the drug with the incorporated components. Further, saturation solubility study revealed increased solubility of the LUF nanosuspension (1670 µg/mL) when compared to the pure drug (212.33 µg/mL). Further, rate of dissolution of LUF from the nanosuspension formulations were found to be significantly (*p* < 0.05) higher when compared to the pure drug. Fabricated lyophilized nanosuspension was found to be stable at 25 ± 2 °C/60 ± 5% RH and 40 ± 2 °C/75 ± 5% RH for the duration of three months. In conclusion, lyophilized nanosuspension showed ~8-folds increase in drug release, which indicated a better way to offer higher release of LUF in controlling malaria.

### ARTICLE HISTORY

Received 13 September 2020  
Accepted 28 December 2020

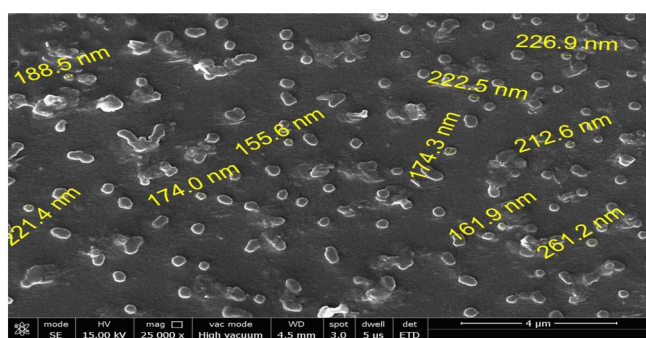
### KEYWORDS

Lumefantrine;  
Nanosuspension; Oral  
bioavailability; solubility;  
drug delivery; anti-  
malarial agent

**CONTACT** Prashant Kesharwani  [prashantdops@gmail.com](mailto:prashantdops@gmail.com)  Faculty of Pharmacy, School of Pharmaceutical Education and Research, Jamia Hamdard, New Delhi 110062, Delhi, India; Tejal Soni  [tejalsoni.ph@ddu.ac.in](mailto:tejalsoni.ph@ddu.ac.in)  Dharamsinh Desai University, Nadiad, Gujarat, India.

© 2021 Informa UK Limited, trading as Taylor & Francis Group

## GRAPHICAL ABSTRACT



SEM images of Lyophilization of LUF nanosuspension formulation

## 1. Introduction

Malaria is a life-threatening disease caused by *Plasmodium* parasites, where the infected carriers, particularly female Anopheles mosquitoes, transmit the infection from person-to-person [1]. According to the estimation by World Health Organization (WHO), 228 million cases of malaria infections were made, where the death penalty was paid by 405,000 numbers of patients in 2018 [2]. This is a common disease in the developing countries and to prevent it, several measures are taken by the governing authorities. The control of this disease is possible with proper treatment following prompt diagnosis. Emergence of need for the treatment of the protozoa, there are several strategies available, from chloroquine to artemisinin-based combination therapies [3,4]. However, quinine categories are found to be unsuccessful due to the uneven dosage schedule and unsatisfactory bioavailability [5]. Additionally, combination of artemether and lumefantrine (LUF) are known to provide better control over the malarial condition [4].

Among the combination of artemether-LUF, the latter is a lipophilic drug, chemically it is tertiary amine and fluorene member. Some of the literature had categorized this drug under the class II of Biopharmaceutical Classification System (BCS) [6], where some has categorized under class IV drug [7]. LUF acts as a blood schizonticide, causes inhibition of heme detoxification process, which makes heme toxic and induce free radicals. Finally, these free radicals lead to death of the parasite [8,9]. Even though it is a very effective compound in the treatment of malaria, its activity and clinical therapeutic effect are limited due to poor aqueous solubility of LUF. Oral bioavailability of this drug is only 4–11%, where the variability in oral bioavailability is due to the influence of concomitant fatty food consumption [10]. The necessary blood level of the LUF could be achieved for therapeutic efficacy when LUF is administered with fatty food, thereby bioavailability of the drug can be improved. However, this fat food dependent increase in oral bioavailability of LUF is illustrated higher extent of variation in different volunteers [11]. The high log P value of LUF (9.35)

indicates its' hydrophobic nature, thus researchers are attempting to improve the bio-availability of this drug using novel approaches. Many techniques had been reported in the literature toward increase in solubility and/or bioavailability of LUF, such as formulating solid dispersion using Kollidon VA 64® [12], solid-lipid nanoparticles [13], self-nanoemulsifying ionic complex [14], nanostructured lipid carriers [15], nano-liposome [16], amorphous solid-dispersion granules [17], etc. Due to lower percentage of drug loading, lower stability, high manufacturing cost and increased number of steps in manufacturing for above cited techniques limit its application in preparation of viable formulation of the drug at an economic level.

Thus, the present research is attempted to develop nanosuspension of LUF with the aim to formulate a novel delivery system of LUF to possess improved solubility and bioavailability in a cost effective manner [18]. However, these nanosuspension dosage forms are known to possess physical instability due to agglomeration of the particles of nanometer range [19]. This stability problem of nanosuspension could be overcome by utilization of an appropriate stabilizer. The stabilizers, may be nonionic polymers (like polyvinylpyrrolidone (PVPK30), polyvinyl alcohol (PVA) and hydroxypropyl methylcellulose (HPMC)) or non-ionic surface-active agents (like Poloxamer 188 and Polysorbate 80) or ionic surface-active agents (like sodium lauryl sulfate (SLS)) [20]. Alternatively, drying of nanosuspensions can also be employed for stabilization of the nanosized drug particles. Thus, nanosuspension could be dried either by lyophilization or by spray drying technique to prolong stabilization of the formulations [21]. Therefore, it is mandatory to consider these factors while fabricating a stable nanosuspension with uniform particle size without having large differentiation between their sizes. This may help to avoid different saturation solubility levels and dissimilar concentration gradients, and will also direct to stop the phenomenon of Ostwald ripening [22]. Therefore, the present research work has been attempted to incorporate soya lecithin for its beneficial role on facilitating lipids-based drug absorption. Further, freeze-drying was employed for drying of the nanosuspension formulation followed by stability measurement, *in vitro* assessment of release profile and antimalarial efficacy.

## 2. Materials and methods

### 2.1. Materials

LUF was procured as gift sample from Mangalam drugs and Organics, India. Soya lecithin (LECIVA S12 NF) was gifted from VAV Life Sciences Limited, Mumbai, India. PVPK30 was obtained from Anshul Life Sciences, India. HPMC E5 was purchased from Dow Chemicals, Michigan, USA. Poloxamer 188 and Polysorbate 80 were procured from Sigma Aldrich, USA. HPLC grade chloroform was obtained from Merck, Mumbai, India. Ultra-pure deionized water was prepared from a Millipore Milli-Q Gradient system, Bedford, USA. All other chemicals and solvents utilized were of analytical grade.

**Table 1.** Composition of different formulated complexes of lumefantrine.

Complex	LUF (mg/g)	Soya lecithin (mg/g)	PVPK30 (mg/g)
Complex 1 (1:1:1)	333.333 mg	333.333 mg	333.333 mg
Complex 2 (1:2:1)	250.0 mg	500.0 mg	250.0 mg
Complex 3 (1:3:1)	200.0 mg	600.0 mg	200.0 mg
Complex 4 (1:4:1)	166.7 mg	666.8 mg	166.7 mg

LUF: Lumefantrine, PVPK30: polyvinylpyrrolidone.

## 2.2. Experimental methods

### 2.2.1. Selection of solvent for LUF

Selection of suitable solvent system for the preparation of nanosuspension was carried out by analyzing solubility of LUF in different solvent system. Thus, solubility of LUF was determined in acetone, chloroform, dichloromethane, dimethylformamide, methanol, ethanol and dimethyl sulfoxide.

### 2.2.2. Preparation of LUF: soya lecithin: PVPK30 complex (LSP-C)

From the review of literature, it was established that in presence of fatty food promotes solubility of LUF, and thus bioavailability. Hence, complex formation was carried out with different ratio of the drug, soya lecithin and PVPK30 (1:1:1, 1:2:1, 1:3:1 and 1:4:1, respectively). The composition of different complexes was summarized in Table 1. Solubility of LUF for each ratio was determined and ratio that showed maximum drug solubility was selected to prepare the nanosuspension.

For complex preparation, LUF and PVPK30 was dissolved in chloroform by continuous stirring for a duration of 15 min using magnetic stirrer at 600 RPM. In the next phase, required quantity of soya lecithin was dissolved in chloroform by continuous stirring for 15 min at 600 RPM using magnetic stirrer. Then, mixture of drug and PVPK30 was gradually added to the solution of soya lecithin with continuous stirring at 800 RPM for 15 min. Once the clear dispersion was obtained, the organic solvent (chloroform) was evaporated using rotavapor. Finally, the dried complex was used to formulate the nanosuspension.

### 2.2.3. Preparation of LUF nanosuspensions

LUF nanosuspensions were prepared using anti-solvent precipitation and ultrasonication technique. Solvent phase for nanosuspension preparation was fabricated by dissolving LUF-soya lecithin complex (LSP-C) in chloroform. Inclusion of soya lecithin, the mixture of phospholipids from natural sources, plays important roles toward improvement of stability of the nanosuspension and simultaneously aids in solubility improvement of the drug. Therefore, soya lecithin was incorporated in the present experiment toward improvement of stability of the formulation since it has been widely incorporated in the complexation process and established as a good dispersant and surfactant [23]. Additionally, incorporation of soya lecithin could promote strong enthalpic interaction between the solvent and stabilizer, which in process, induces steric repulsion and prevent agglomeration of the suspended nanoparticles [24].

On the other hand, the anti-solvent phase was prepared by dissolving HPMC-E5 (1% w/v), Poloxamer 188 (1% w/v) and Polysorbate 80 (0.5% w/v) in Milli-Q water. Polymeric surfactants (e.g. HPMC, Poloxamer, PVPK30, etc.) are usually employed to

stabilize the nanosuspensions. Soluble polymer, such as PVPK-30, is known to exert dual function in the formulation; firstly, act as a stearic stabilizer by adsorption on nanoparticles surface; secondly, retards aggregation due to slower Brownian motion during storage, as well as phase separation-induced aggregation during drying [25].

On the other hand, studies reported in literature suggests that the combination of surfactant (e.g. Polysorbate 80) and polymers in the nanoformulations offers greater stability of the final product, which will prevent aggregation by facilitating steric hindrance or by the electrostatic repulsive effect, thereby maintains the quality of the product for longer period [26].

In the next step, the solvent phase containing drug was gradually added to the anti-solvent phase using syringe drop wise. The mixture of solvent and anti-solvent phase was homogenized at a speed of 10,000 RPM using high-speed homogenizer (Ultraturax, IKA). The temperature of aqueous phase was maintained at 2-8 °C during stirring for immediate precipitation to prevent growth of crystals and to get a uniform size distribution of particles. After complete removal of chloroform, Dispersion was further sonicated using probe sonicator (Sonics) for 15 min at 30% amplitude at 2-8 °C.

#### **2.2.4. Optimization of nanosuspension formulation**

Design of Experiment (DoE) is an element of Quality by Design (QbD) approach and applied to reduce number for experimental run and to improve finished product quality. Design Expert<sup>®</sup> 11.0 was used to generate response surface plots and to optimize the formulation. A 3<sup>2</sup> full factorial design was utilized to optimize the critical factors in formulation. As per the design, concentration of surfactant (Polysorbate 80) (X<sub>1</sub>) and sonication time (X<sub>2</sub>) were selected as independent variables. While mean particle size (nm) (Y<sub>1</sub>) and drug release after 90 min (t<sub>90</sub>) (Y<sub>2</sub>) were selected as dependent variables and experimental runs as per the DOE was performed. For all the responses, polynomial equations were generated which includes linear, interaction and quadratic terms. Choice of the best fitting model was derived upon several statistical parameter correlations, including adjusted regression coefficient (adj. R<sup>2</sup>), coefficient of variation (CV) and regression coefficient (R<sup>2</sup>). For optimization, equation of mathematical model linking independent variables and their interactions for different quantified responses derived for 3<sup>2</sup> factorial design is:

$$Y = b_0 + b_1X_1 + b_2X_2 + b_{12}X_1X_2 + b_{11}X_1^2 + b_{22}X_2^2$$

Where, Y is the value of dependent variable, b<sub>0</sub> is overall coefficient, and b<sub>1</sub> and b<sub>2</sub> are the coefficient of X<sub>1</sub> and X<sub>2</sub>.

Response surface plots were plotted to establish the relationship between independent and dependent variables [27].

#### **2.2.5. Lyophilization of LUF nanosuspensions (LP-NS)**

Optimized nanosuspension was formulated and was lyophilized to get dry powder form. 2 mL of nanosuspension was filled in clear glass vials and stoppered for freeze-drying. The batches were pre-freeze at -25 °C prior to sublimation and desorption. After freezing, sublimation commenced at 15 °C at 200 mT pressure for variable time

periods throughout the process. Finally, secondary drying was performed at 35 °C for 30 h under 50 mT vacuum. LP-NS formulations were kept in the properly sealed vials at room temperature until further use. A 2% *w/v* mannitol was added to the formulation as a cryoprotectant to prevent agglomeration of nanoparticles and to stabilize the nanosuspension formulation.

### **2.2.6. Re-dispersibility of LP-NS**

Evaluation for the re-dispersibility of the LP-NS was performed following methods reported by Mauludin and team [28]. A quantity of 100 mg of the lyophilized nanosuspension was taken in a glass vial and 2 mL of water was added into that. Later, the vial was inverted 3 to 4 times until sediment was uniformly dispersed. After uniform dispersion, the particle size, PDI, and surface charge of the dispersion were studied and compared with freshly prepared optimized nanosuspension.

### **2.2.7. Residual solvent analysis**

Presence of chloroform as residual solvent in LP-NS was investigated using gas chromatography (GC). The system utilized was an Agilent 7820 A with a capillary column and flame ionization detector. A 75 mg of lyophilized sample was dissolved in 4 mL N,N-dimethyl formamide after accurately weighing. A 2 mL of the solution was instilled into the GC system at 3.5 mL/min flow rate with nitrogen as carrier gas. Oven temperature was controlled at 110 °C, injector was set at 200 °C and detector temperature was set at 250 °C.

### **2.2.8. Saturation solubility study**

Saturation solubility was performed to establish aqueous solubility of pure LUF, LSP-C and LP-NS. Thus, it was determined in different aqueous buffer medium of pH 1.2, pH 7.4, pH 6.8 and pH 4.5. An excess amount of sample was added in different medium and shaken using orbital shaker incubator (Heathrow scientific, USA) at 37 °C at 200 rpm for 48 h. The samples were centrifuged (REMI Instruments, India) at 5,000 rpm for 15 min and filtered using 0.22 µm syringe filter. Samples were analyzed using UV spectrophotometer at  $\lambda_{\text{max}}$  of 235 nm.

### **2.2.9. Analysis of zeta potential, particle size and polydispersity index (PDI)**

Zeta potential and average particle size were determined by Malvern ZetaSizer (Nano ZS90 series UK) functioning based on dynamic light scattering principle [29]. A 100 mg of lyophilized sample was re-dispersed in 2 mL of Milli-Q water and mixed to achieve a uniform sample dispersion. A 100 µL of sample was transferred into a test tube and diluted up to 4 mL using Milli-Q water and analyzed immediately at room temperature. All measurements were made in triplicate.

### **2.2.10. Differential scanning calorimetry (DSC) study**

DSC was performed to evaluate interactions between LUF and incorporated excipients. DSC Q2000 (TA Instruments) was utilized for the study. Each sample was weighed 3 mg (Pure LUF, LSP-C and LP-NS) and was heated in aluminum pans for 10 °C/min from 25 °C to 300 °C.



### **2.2.11. X-ray powder diffraction (XRPD) study**

XRPD analysis is useful to analyze physical state of the formulation. XRPD diffractograms for the pure LUF, LSP-C and LP-NS were determined using Xpert, Philips, Holland. Exact quantity of the sample for the analysis was pressed to incorporate into the sample holder. The X-ray radiation source was a Cu/Ni in the instrument, which was operated at 40 kV. Other set parameter for the analysis were at 5° to 50° 2 $\theta$  series, for a 2°/min scanning rate.

### **2.2.12. Fourier transform-infrared (FT-IR) spectroscopy study**

FT-IR study of the samples was carried out to evaluate any chemical modification in the drug. FT-IR spectrophotometer (Bruker, Switzerland) utilized to analyze the sample spectrum at the wavelength range from 4000 to 400 cm<sup>-1</sup>. Pure LUF, LSP-C and LP-NS were subjected to FT-IR analysis.

### **2.2.13. Proton nuclear magnetic resonance (<sup>1</sup>H NMR) spectroscopy**

Proton NMR spectra of LUF and LSP-C was performed using NMR spectrometer model advance III (Bruker) with <sup>1</sup>H resonance frequency of 500 MHz. Deuterated chloroform was used as solvent for the sample preparation in this analysis.

### **2.2.14. Scanning electron microscopy (SEM)**

Surface morphology of LP-NS was evaluated using SEM. SEM analysis of the samples was performed by using field emission SEM (Quanta 400 F) at 2–20 kV acceleration voltage. Before scanning, samples were coated with gold-palladium.

### **2.2.15. Stability study**

Wet nanodispersions were collected after ultrasonication. Stability study of wet nanodispersion and LP-NS formulations were carried out by keeping sealed vials in a stability chamber under specific condition. Samples were evaluated for dispersed particle size over a period of 3 months, where sampling was made at 1, 2, and 3 months. Particle size determinations were executed in triplicate.

### **2.2.16. In vitro dissolution study**

*In vitro* release study of LP-NS, pure LUF and marketed dry syrup containing LUF was carried out using USP type II (paddle type) dissolution apparatus following dialysis bag method [30]. 0.1 N hydrochloric acid (pH 1.2) containing 0.5% (w/v) sodium dodecyl sulfate (SDS) was used as dissolution medium. 5 mL samples were withdrawn at different time points (10, 15, 30, 45, 60, 90 and 120 min) and restored with 5 mL of fresh dissolution medium. The dissolution study was carried out at 50 rpm at 37°C ± 0.5°C. All samples were analyzed in triplicates using UV spectrophotometer at  $\lambda_{\text{max}}$  235 nm.

### **2.2.17. In vitro antimalarial assay**

Antimalarial assay was performed *in vitro* against chloroquine sensitive *P. falciparum* 3D7 strain. *P. falciparum* 3D7 culture was maintained *in vitro* as described in the literature [31] consisting of RPMI 1640 powdered medium supplemented with Hepes



buffer (25 mM) and 0.2% NaHCO<sub>3</sub> (hereafter abbreviated as RP) with 10 percent type AB human serum and heparin solution (30 mg of heparin per 100 mL of blood in 0.85% NaCl) equivalent to one-tenth the volume of the re-suspended cells. Stock solution of the formulation was prepared by dissolving specific amount of methanol and benzalkonium chloride (BKC) in 0.05 N HCl. For the determination of 50% inhibitory concentration (IC<sub>50</sub>), dilutions of the stock solution were made with sterile distilled water. The final concentrations ranged from 1 to 70 ng/mL for pure LUF powder and marketed dry syrup. The final concentrations ranged from 0.19–48 ng/mL for LP-NS (equivalent to 0.05–12.8 ng/mL for LUF) were distributed in a 96 well plate. The standard anti-malarial agent, chloroquine was incorporated in the present experiment as the positive control to compare the efficacy of the test and marketed formulations of LUF. Asynchronous culture of the parasite (~2–3% parasitemia and 2–3% hematocrit) was exposed to the drug dilutions for 72 h. (37 °C, 5% CO<sub>2</sub>). Lytic buffer (20 mM Tris pH 7.5, 5 mM EDTA, 0.008% saponin, and 0.08% triton X-100) containing SYBR green-I was added to each well and incubated for 3 h at room temp in dark. The mean parasitemia was calculated from the triple-read replicate test. The mean parasitemia in the drug-free control wells served as the parameter of optimum and relative growth inhibition in the drug wells and was calculated based on formula as suggested by Fidock et al. [32]. Plates were read under fluorescence reader (excitation at 485 nm and emission at 535 nm). IC<sub>50</sub> was determined based on DNA content of the parasite [33].

$$\text{Activity} = \frac{100 - \text{mean parasitemia treated}}{\text{mean parasitemia control}} \times 100$$

### 3. Results and discussion

#### 3.1. Selection of suitable organic solvent

Selection of suitable solvent is an important process for fabricating a suitable nano-suspension, as it is desired to provide goods solubility. For this study, solubility of LUF was measured in different solvents like acetone, chloroform, dichloromethane, dimethylformamide, methanol, ethanol and dimethyl sulfoxide. Based on the results of the study, chloroform was selected as solvent for LUF due to highest solubility of drug (106 mg/mL) when compared to other tested solvents (Figure 1(a)).

#### 3.2. Selection of LUF-Soya lecithin complex

LUF, soya lecithin and PVK30 complex was prepared in different ratio of the components, 1:1:1, 1:2:1, 1:3:1 and 1:4:1, respectively. Suitable ratio was selected on the basis of aqueous solubility of complex using saturation shake flask method. Among all the four complexes prepared, 1:4:1 (LUF: Soya lecithin: PVPK30) indicated highest solubility in water (921 µg/mL) (Figure 1(b)). Whereas, the other ratios (1:1:1, 1:2:1 and 1:3:1) showed the solubility of 615 µg/mL, 746 µg/mL and 830 µg/mL, respectively. Hence, the 1:4:1 ratio was selected for preparation of nanosuspensions.

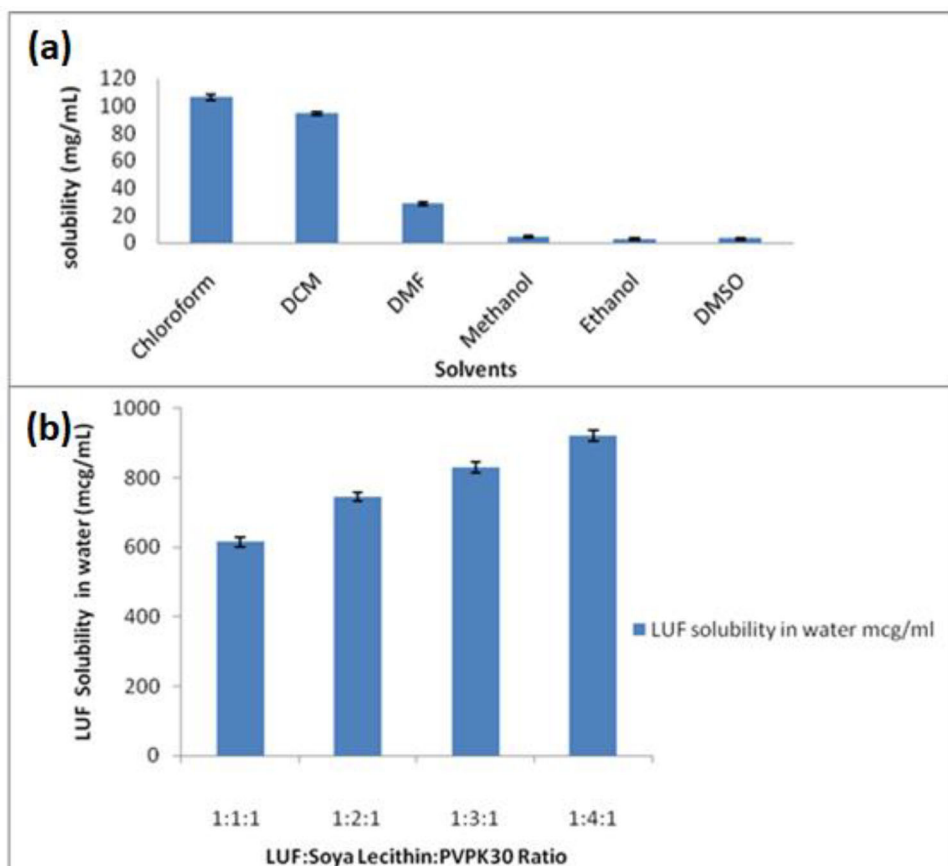


**Figure 1.** Saturated solubility of LUF in different solvents; (b) Selection of Ratio of LUF: Soya lecithin: PVPK30.

### 3.3. Preparation of nanosuspension

Finally, the nanosuspension of LUF was prepared using solvent-antisolvent technique as described earlier. Nanosuspension experiment was designed as per  $3^2$  full factorial design as per DoE (Table 2). Result of the experimental runs is presented in Table 3.

### 3.4. Optimization of nanosuspension

Nanosuspension formulation was optimized by using DoE software, where concentration of surfactant ( $X_1$ ) and sonication time ( $X_2$ ) were selected as independent variable, while particle size and  $t_{90}$  was selected as dependent variable. Responses obtained as per DoE were analyzed using multiple linear regression analysis (MLRA) and ANOVA and polynomial equation for each response variable was derived. Model was designed at  $p < 0.05$ .

#### 3.4.1. Optimization of particle size

Particle size of all 13 batches are presented in Table 3. Effect of  $X_1$  and  $X_2$  on particle size was presented in contour plot and 3D response surface plot (Figure 2(a,b)).

**Table 2.** Experimental runs for preparation of nanosuspension as per 32 full factorial design.

Batch no	Coded independent variable		Actual Value	
	Concentration of Polysorbate 80 (X1) (% w/v)	Sonication time (X2) (min)	Concentration of Polysorbate 80 (X1) (% w/v)	Sonication time (X2) (min)
F1	+1	-1	1	15
F2	0	-1	0.625	15
F3	+1	0	1	22.5
F4	0	0	0.625	22.5
F5	-1	+1	0.25	30
F6	0	0	0.625	22.5
F7	0	0	0.625	22.5
F8	0	0	0.625	22.5
F9	-1	-1	0.25	15
F10	+1	+1	1	30
F11	0	0	0.625	22.5
F12	0	-1	0.625	30
F13	-1	0	0.25	22.5

**Table 3.** Results of experimental runs for preparation of nanosuspension.

Batch no	Particle size (nm) (Y1)	T90 (Mins)
F1	117.94	12
F2	237.18	24
F3	95.34	3
F4	165.56	15
F5	208.9	15
F6	165.56	15
F7	154.45	12
F8	146.57	12
F9	384.82	36
F10	111.98	6
F11	140.76	15
F12	129.34	6
F13	221.45	18

From the presented results, it is indicated that there is increase in surfactant concentration with simultaneous increase in sonication time there is decreased particle size. A polynomial equation (1) derived from the MLRA and ANOVA is presented as follow:

$$\text{Particle size (nm)} = +151.98 - 81.65X_1 - 48.29X_2 + 42.49X_1X_2 + 12.91 X_1^2 + 37.37 X_2^2 \quad (1)$$

According to the Equation (1) mentioned above, the negative values of coefficient indicates negative impact and vice versa. Concentration of surfactant had negative impact on the particle size, i.e. an increase in the concentration of surfactant will increase particle size. The time of ultrasonication showed a marked effect on particle size. Particle size for nanosuspension was increased with increased time of ultrasonication. Our results are well in accordance with previous report available in the literature [34]. The application of ultrasonic energy could generate high-energy ultrasonic waves. These shock waves could reduce the contact time between the particles and thereby, prevent the agglomeration of the particles. The ultrasonic waves also could increase the adsorption of polymers on the particle surface and simultaneously cause the disruption of agglomerates. However, longer duration of ultrasonication did not

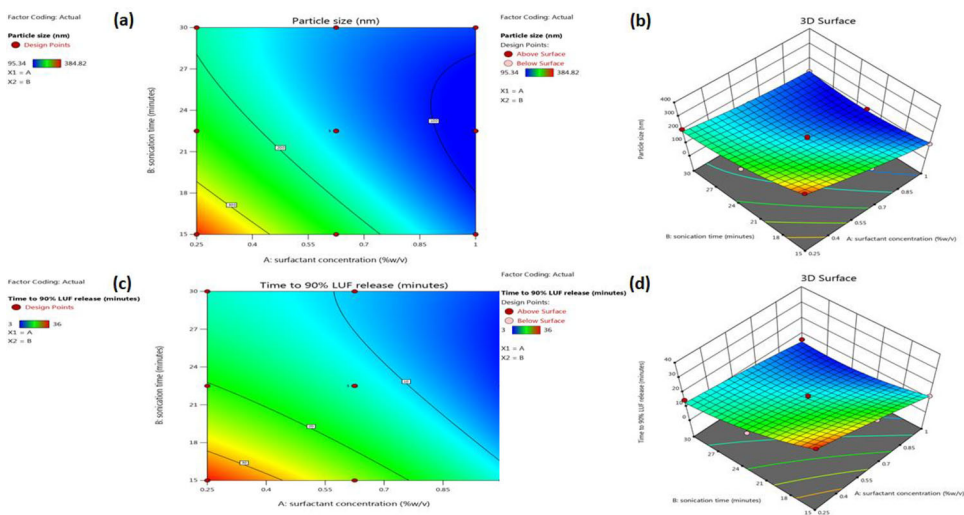


**Figure 2.** (a) Contour plot showing effect of X1 and X2 on particle size; (b) 3D response surface plot showing effect of X1 and X2 on particle size; (c) Contour plot showing effect of X1 and X2 on  $t_{90}$  (d) 3D response surface plot showing effect of X1 and X2 on  $t_{90}$ .

help in reduction of particle size, because it may cause the disruption of the adsorbed polymeric film, which might lead to the agglomeration of particles. Hence, in our present experiment, the process of probe sonication for shorter duration obtained nanosized and homogenous particles of the nanosuspension.

### 3.4.2. Optimization of $t_{90}$

Effect of  $X_1$  and  $X_2$  on  $t_{90}$  is illustrated in Figure 2(c,d). The results showed that the increasing in surfactant concentration with increasing sonication time reflected by decreased  $t_{90}$ . A polynomial equation derived from the MLRA and ANOVA was presented as follow:

$$t_{90} = +13.03 - 8.00X_1 - 7.50X_2 + 3.75X_1X_2 - 0.6207X_1^2 + 3.88X_2^2 \quad (2)$$

The decreased dissolution rate of LUF might be due to its larger crystal size and lower aqueous solubility. This was further confirmed through its distinctive peaks using both XRPD and DSC techniques. Increased rate of drug release from the nanosuspension might be due to various possibilities; such as (a) presence of polymers with high hydrophilic property that result into reduction of aggregation and enhancement in wettability of drug; (b) reduction of LUF crystallinity in nanosuspensions, thus an amorphous LUF showed an elevated thermodynamic activity when compared to crystalline LUF, which lead to faster release; (c) reduction in particle size of the LUF leading to increased surface area and ultimately increase the dissolution of drug. The variability in drug release profile might be due to variation in particle size of nanosuspension formulation.

Amongst all the tested formulations, batch F3 illustrated the minimum mean particle size i.e. 95.34 nm, with the lowest  $t_{90}$  (3 min); hence, F3 was selected as optimized batch of nanosuspension formulation for further experimentation.

### 3.5. Lyophilization of optimized nanosuspension

Lyophilization is the process by which one can get a free-flowing powder formulation of the LUF nanosuspension. Batch F3 was lyophilized and it was evaluated for different parameters.

### 3.6. Characterization of LP-NS

#### 3.6.1. DSC study

DSC thermograms of the LUF, soya lecithin, PVPK30, LSP-C, LP-NS and the marketed formulation (dry syrup) of LUF are illustrated in Figure 3(a–f). Presence of endothermic peak at 133.6 °C in the thermogram of DSC indicated melting point of LUF as showed in Figure 3(a), which is identical to the reported peak for LUF. DSC thermogram LUF: LSP-C showed that the melting starts at 87.38 °C to 143.69 °C, indicating that complex was successfully formed as depicted in Figure 3(d) [35]. DSC thermogram of LP-NS endothermic peak at 44.52 °C starting at 39.01 °C, might have resulted from the melting of Poloxamer 188 in the formulation, slightly shifted to lower side to actual melting point at 53.49 °C [36].

Further, DSC thermogram of lyophilized nanosuspension showed absence of identical peak of LUF as displayed in Figure 3(e). This indicates successful complex formation and absence of free drug in crystalline form during lyophilization process. Presence of endothermic peak at 150.02 °C in the thermogram also indicates melting point of LUF and 115.28 °C indicates melting point of artemether in the marketed formulation (dry syrup) indicates crystalline nature of LUF (Figure 3(f)). Alternatively, disappearance of the melting endotherm of LUF in the DSC thermogram of LSP-C and LP-NS suggested that drug has been converted to amorphous form when fabricated. High-energy input during the nanonization might induce the changes in the crystalline state of the drug, which could possibly lead to the conversion to amorphous structure [37].

#### 3.6.2. Re-dispersibility of LP-NS

Zeta potential is an evaluation of electrostatic stabilization and plays a vital function for the nanosuspension stability. The formulation was found to be quite stable as portrayed by stability data of the samples stored at different temperature conditions. This could be explained by the fact of nonionic surfactants utilization in the formulation leading to lower zeta potential values to accomplish further stability in physical form. Particle size, PDI and zeta potential of the optimized LP-NS was found to be  $168.3 \pm 1.8$  nm, 0.126, and  $-25.7 \pm 0.9$  mV, respectively (Figure 4(a,b)). Results indicated a uniform colloidal system and good colloidal stability (Table 4).

#### 3.6.3. X-ray diffractogram (XRPD) studies

XRPD is useful method for the detection of compound complexation in powder or microcrystalline states. The diffraction pattern of the complex is supposed to be clearly distinct from that of the superposition of each of the components [38]. Therefore, to confirm crystalline state of LSP-C and LP-NS, XRPD study was performed with the same batch of samples that were evaluated using DSC. X-ray

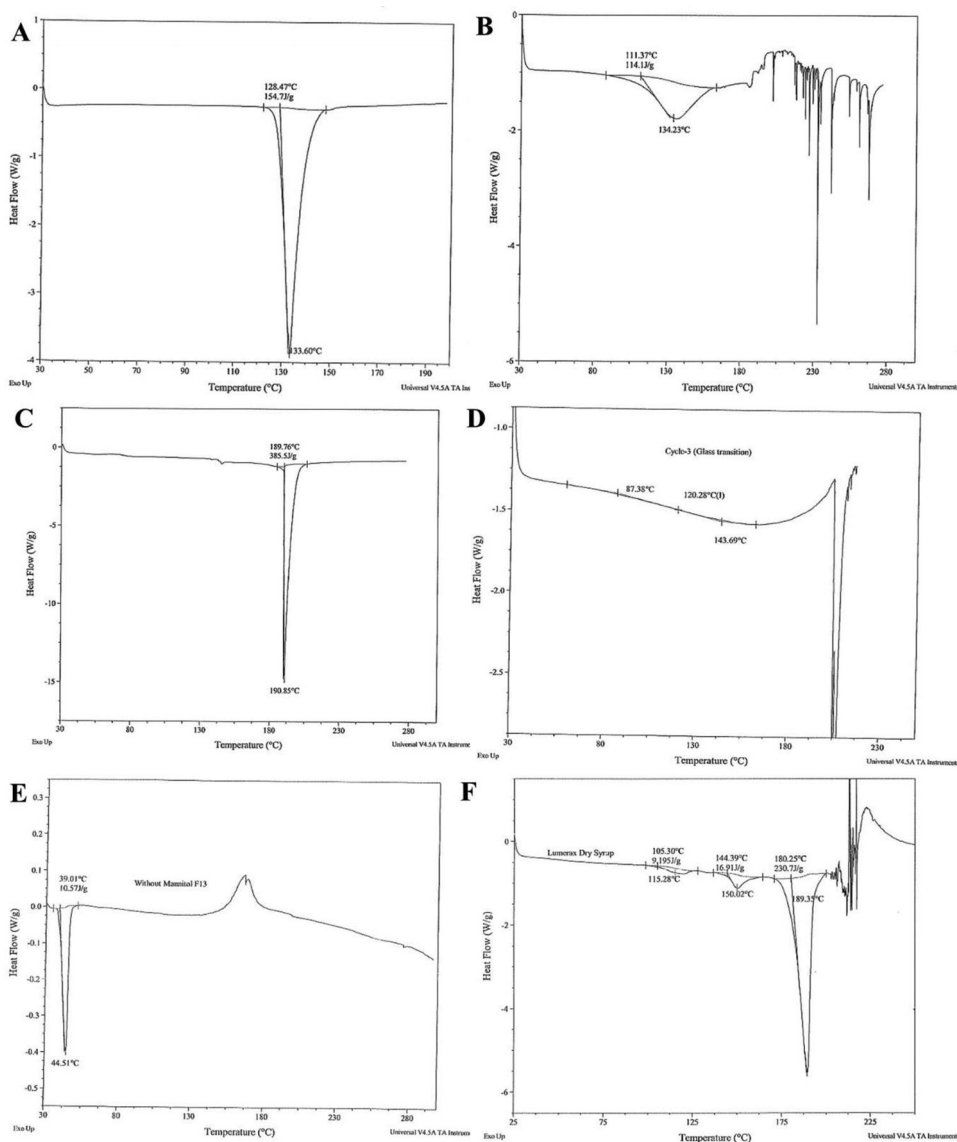


**Figure 3.** DSC thermograms of (a) LUF; (b) Soya lecithin; (c) PVPK30; (d) LSP-C; (e) LP-NS; and (f) marketed dry syrup.

diffraction peaks for pure drug LUF at  $2\theta$  values are of 11.03, 20.06, and 23.01 across the selected region showed sharp, intense and distinct peaks, indicated pure LUF was in the crystalline form, which might lead to poor water soluble property of LUF (Figure 5(a)). However, numbers of LUF characteristic peaks are found to be decreased or disappeared in LSP-C (Figure 5(b)), specifically the peaks at 15.18°, 21.68°, 25.52°, and 20.24°, when compared to that of the pure LUF. This could be said that the crystalline peaks of LUF were disappeared in the complex. This suggests that LUF in the lecithin matrix was molecularly dispersed. XRPD analysis of LUF: LSP-C showed absence of sharp and intense peaks of pure LUF, which revealed

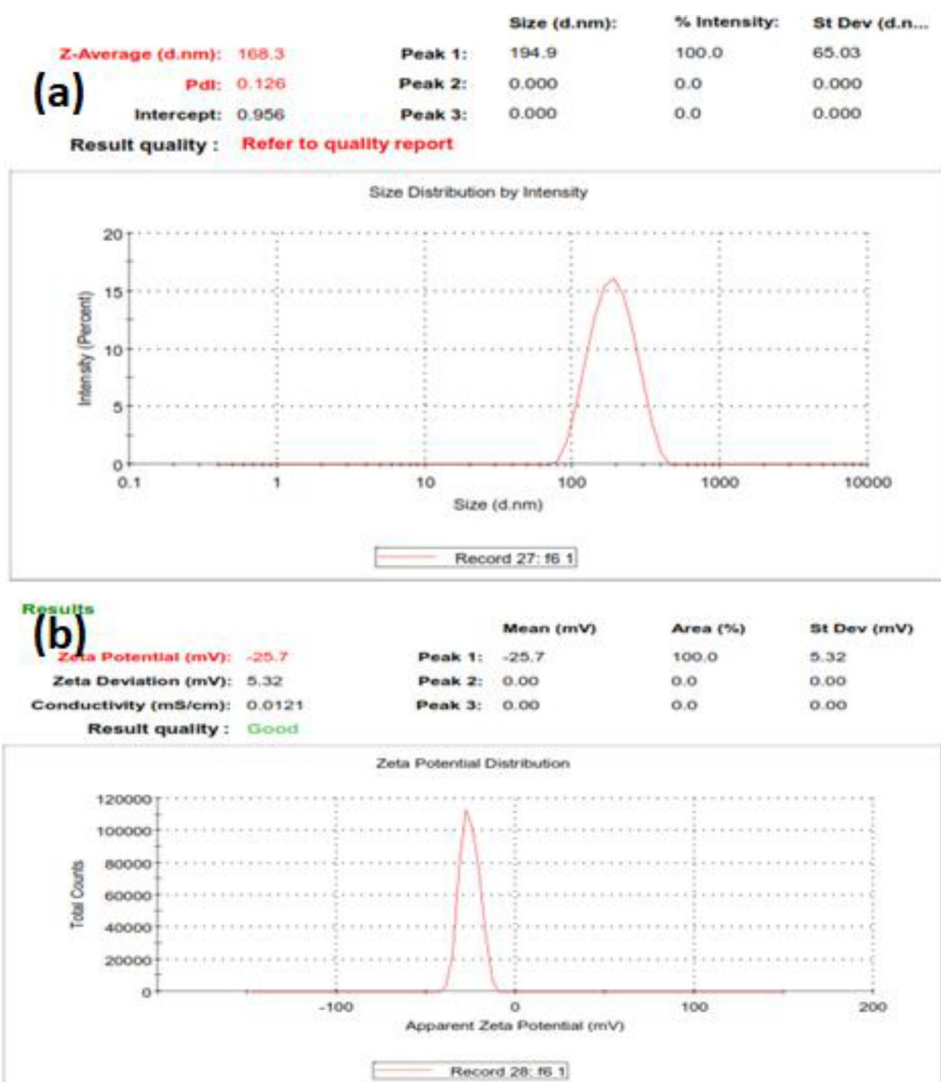


**Figure 4.** (a) Particle size and PDI of re-dispersed LP-NS; (b) Zeta potential of re-dispersed LP-NS.

conversion of crystalline form to amorphous form of drug [39,40]. Alternatively, there are numbers of LUF characteristic peaks decreased or disappeared in LP-NS, specifically the peaks at 11.08°, 26.93° and 25.2°. A large reduction in characteristic peaks indicated the conversion to amorphous nature of LUF. Decrease in the height of peaks of LUF was also observed for LP-NS (Figure 5(c)). This reveals that the crystallinity of LUF was affected by the partial amorphization during the process. Polymorphic transition was not observed as the positions of peaks were comparatively retained in the diffractogram for lyophilized powder. Formation of complex between lecithin and LUF might have lost its crystalline nature and, consequently, the diffraction pattern of the complex, which would not be a simple superposition of those of the two pure components.



**Table 4.** Evaluation of re-dispersed LP-NS.

Parameters	Batch F3	Re-dispersed LP-NS
Particle size (nm) (Mean $\pm$ S. D)	162.25 $\pm$ 1.86	168.3 $\pm$ 1.8
PDI (Mean $\pm$ S. D)	0.153 $\pm$ 0.1	0.126 $\pm$ 0.05
Zeta potential (mV) (Mean $\pm$ S. D)	-25.5 $\pm$ 1.8	-25.7 $\pm$ 0.9

### 3.6.4. FT-IR studies

FT-IR can be performed to determine any chemical modifications of the drug during formulation development. Presentation of FT-IR spectra of the tested samples are displayed in Figure 6. The FT-IR spectrum of LUF showed O-H stretching band near to  $3300\text{ cm}^{-1}$  (Figure 6(a)). Alternatively, in the spectra, the vibrational bands between  $2952\text{ cm}^{-1}$  to  $2870\text{ cm}^{-1}$  of LUF are attributed to linear C-H stretching, whereas the bands at  $1750$  and  $1643\text{ cm}^{-1}$  are due to aromatic  $\text{-C=C-}$  and C-H stretching, respectively. On the other hand, band at  $1155\text{ cm}^{-1}$  represents C-O band vibration, whereas bands at  $873\text{ cm}^{-1}$  and  $770\text{ cm}^{-1}$  are representing the presence of alkanes and  $\text{-C-Cl-}$ . All the significant peaks depicted here for LUF are in agreement to the literature [41]. The FT-IR spectrum of LUF:LSP-C (Figure 6(b)) revealed absence of  $3300\text{ cm}^{-1}$  respective to O-H stretching (Figure 6(b)). This might be due to complex formation at O-H group with soya lecithin, which was further confirmed by C-O-C stretching between  $1000\text{-}1300\text{ cm}^{-1}$  region [42]. Alternatively, the FTIR spectrum of LP-NS (Figure 6(c)) revealed that there was no considerable change in major peaks when compared to FTIR of LSP-C, which confirms that there is no modification or interaction between drugs and excipients.

### 3.6.5. $^1\text{H}$ NMR spectroscopy study

$^1\text{H}$  NMR study was carried out to confirm the complex formation, where the chemical shifts of the proton signals were determined relative to the deuterated chloroform. The  $^1\text{H}$  NMR spectra for LUF displayed specific strong aromatic signals between 7.287 to 7.745 ppm, 2.478 to 2.923 ppm and 0.036 to 1.548 ppm. The results of LUF NMR spectra are in agreement to the reported results in the literature [43]. When compared the spectra of LUF with LSP-C, the signal in  $^1\text{H}$  NMR of LUF (Figure 7(a)) at 4.5 ppm was found to be absent in  $^1\text{H}$  NMR of LSP-C. Further, the signal observed for O-H proton was less intense and broad. The absence of signal in the spectrum of the complex might be explained by the fact of complexation at O-H group in LUF (Figure 7(b)) [44,45].

### 3.6.6. Surface morphology

Optical microscopy of LUF and surface morphology of LP-NS using SEM is illustrated in Figure 8(a,b), respectively. Optical microscopy (Figure 8(a)) of LUF (measured by dispersion of the drug in propylene glycol) clearly indicates crystalline surface and higher range of particle size  $31\text{-}35\mu\text{m}$ . While SEM image (Figure 8(b)) of LP-NS showed remarkable reduction in particle size. Further, spherical shape of the LP-NS could be demonstrated by the covering of the drug particles by HPMC-E5 polymers. Additionally, spherical shape of LP-NS particles revealed the conversion of crystalline form to amorphous form [46].

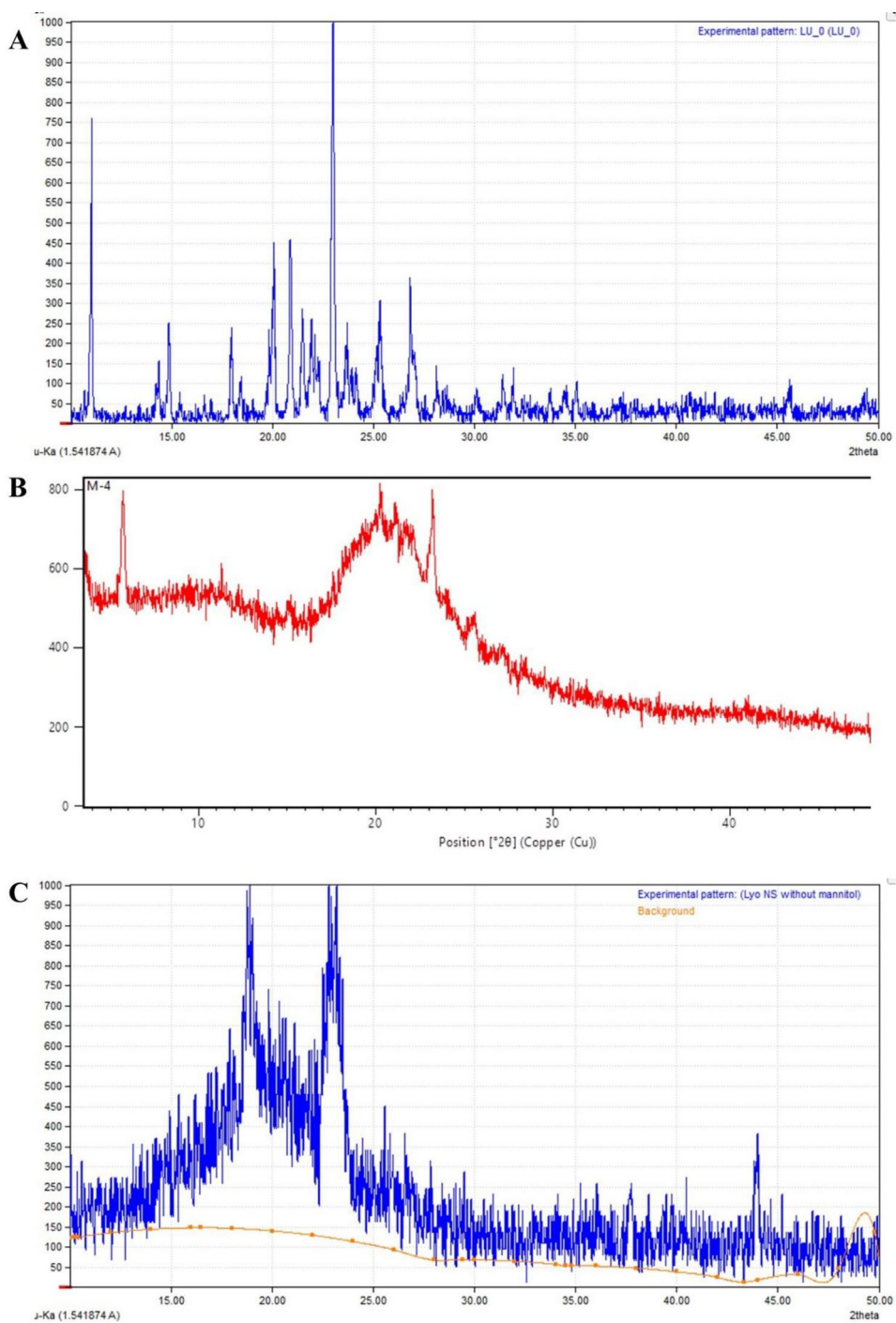
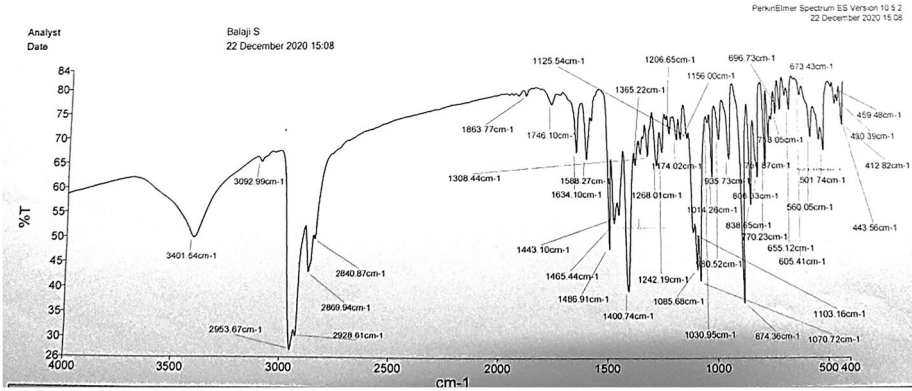


Figure 5. X-ray diffractograms of (a) LUF; (b) LSP-C; and (c) LP-NS.

A



B



C

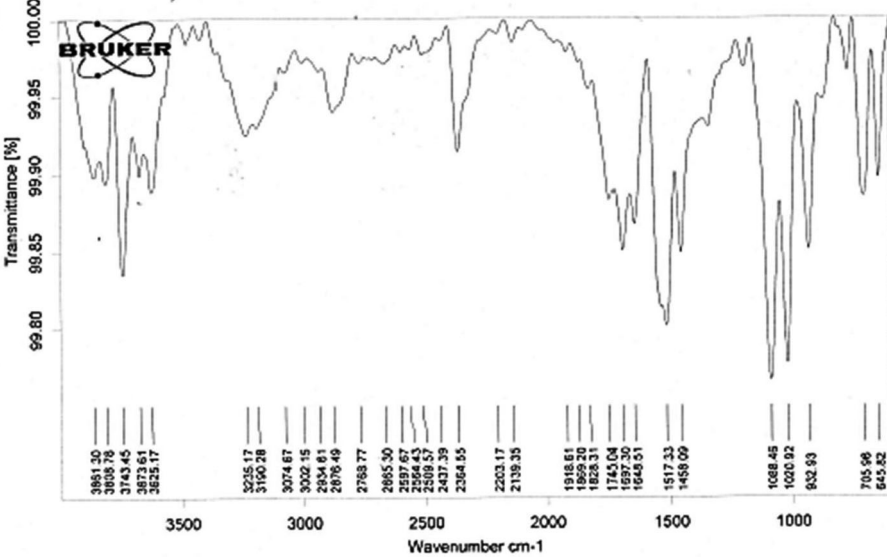
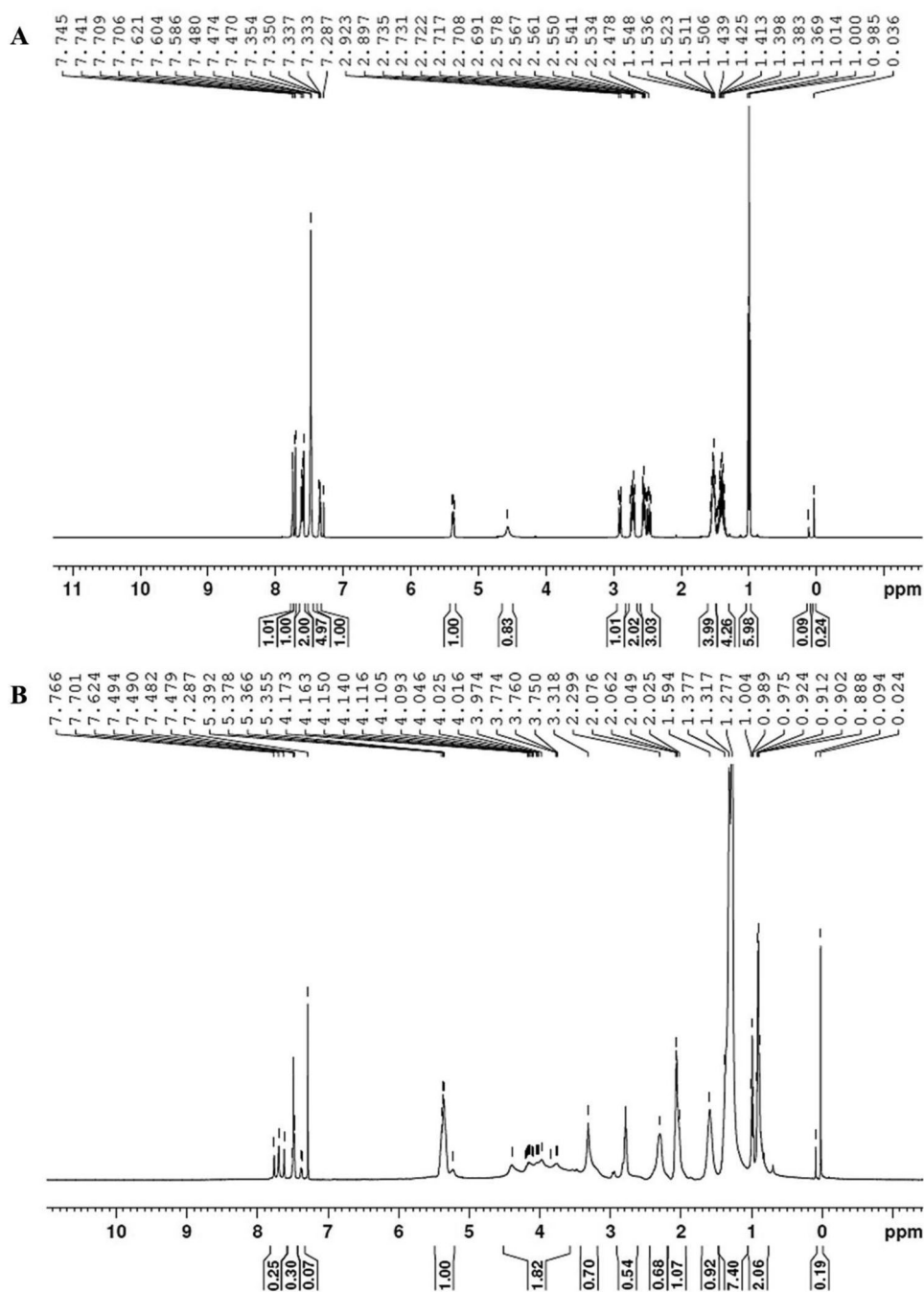


Figure 6. FT-IR spectra of (a) LUF; (b) LSP-C; and (c) LP-NS.



**Figure 7.**  $^1\text{H-NMR}$  spectrum of (a) LUF (b) LSP-C.

### 3.6.7. Saturation solubility studies

The saturation solubility of LUF, LSP-C and LP-NS in water were  $212.33\ \mu\text{g/mL}$  and  $782.66\ \mu\text{g/mL}$  and  $1.67\ \text{mg/mL}$ , respectively. Solubility of LP-NS was distinctly greater

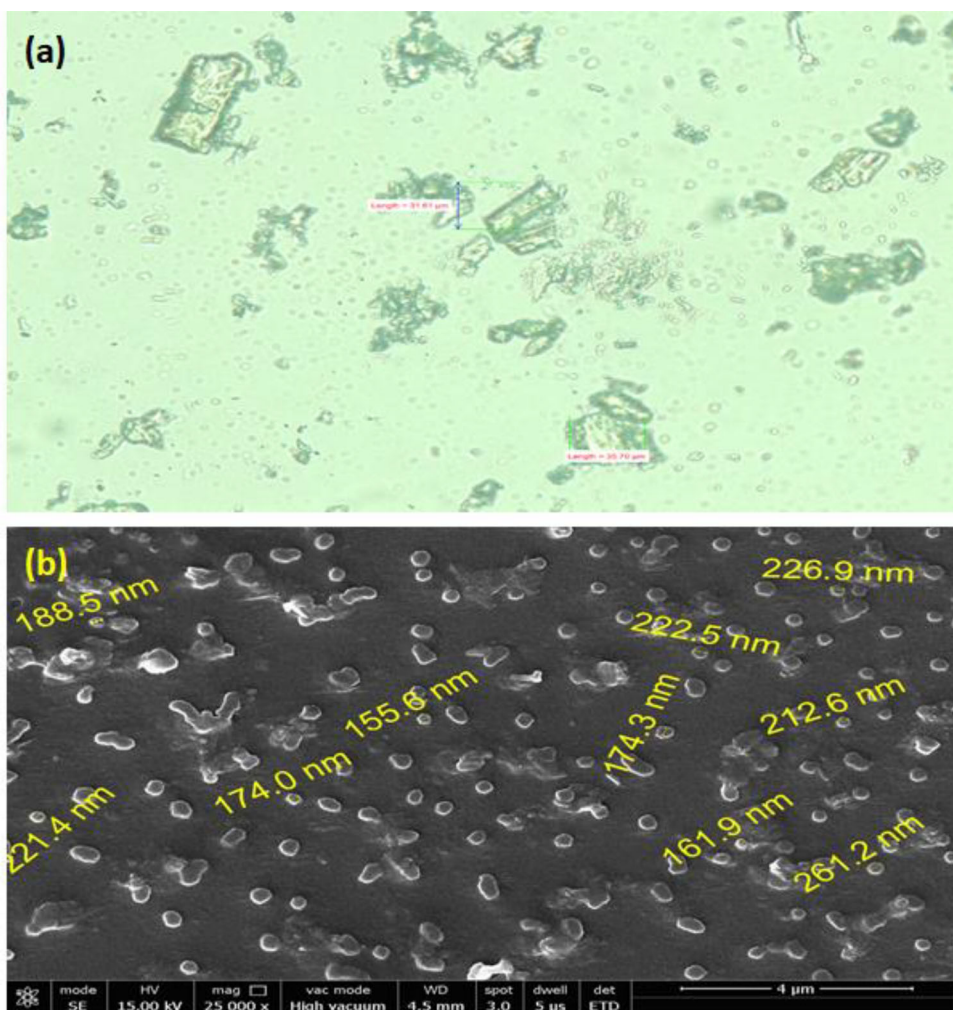


**Figure 8.** (a) Optical microscopy of LUF; (b) SEM images of LP-NS.

than LUF and LSP-C, which further inferred that the lyophilized nanosuspensions could remarkably increase the solubility of LUF (Figure 9(a)).

The results on saturation solubility demonstrated at a function of different pH (1.2, 4.5, 6.8, and 7.4). Solubility study results signify that LUF displayed pH dependent solubility. Unlike pure LUF, unpredictable solubility outcome was achieved for nanosuspension formulations. It is fascinating to make a note of that at pH 1.2, LUF solubility drastically augmented by LSP-C as well as LP-NS.

### 3.6.8. Analysis of residual solvent

Chloroform employed in LUF nanosuspension fabrication fits into class II according to International Conference on Harmonization (ICH) guidelines along with a limits 60 ppm. GC was applied to analyze chloroform level quantitatively in the lyophilized sample. The results of the GC analysis depicted presence of 10 ppm chloroform, which is well below the permitted specifications.



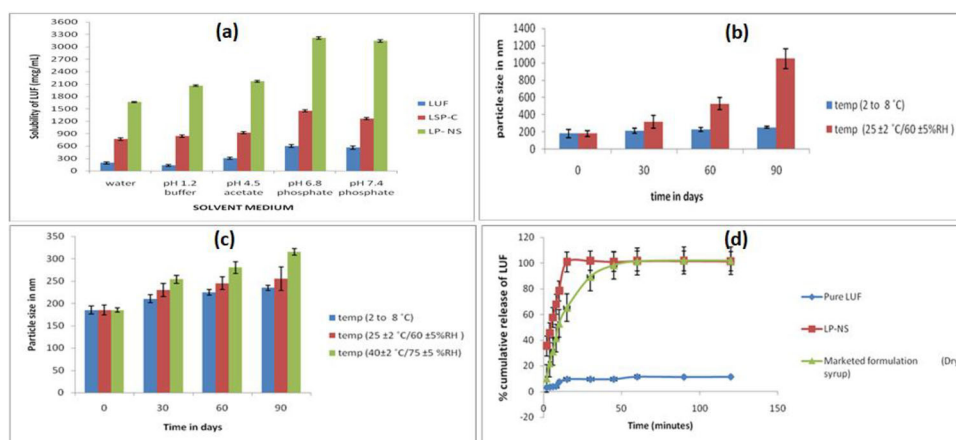


**Figure 9.** Saturation solubility of LUF in water & at different pH; (b) short term physical stability of wet LUF nanodispersion (Before lyophilization); (c) short term physical stability of LP-NS (After lyophilization); (d) In-vitro drug release profile of LUF and LP-NS and marketed formulation (dry syrup).

### 3.6.9. Physical stability

Stability of wet nanodispersion (before lyophilization) and optimized lyophilized LP-NS formulation was investigated at different temperatures and conditions and the observed data are presented in Figure 9(b,c). Nanocrystals typically show an inadequate aqueous state stability, the particles anticipated to aggregate through phenomenon of Ostwald ripening and by the use of attractive inter-particle forces during storage [47]. To scrutinize the influence of temperature on the stability of LUF nanocrystals, particle size of freshly prepared nanocrystals was compared with the samples kept at different temperatures. Short-term stability of wet nanodispersion (before lyophilization) and LP-NS (after lyophilization) was examined in terms of particle size. After 3 month storage of nanosuspensions, there was no noticeable transformation on particle size for wet nanodispersion (before lyophilization) stored at 2 to 8 °C but significant increase in particle size observed at 25 ± 2 °C/60 ± 5%RH, where the size was increased to 1050 nm after 3 months for wet nanodispersion.

Alternatively, after three months storage of LP-NS, no significant changes in particle size was observed at 2 to 8 °C and 25 ± 2 °C/60 ± 5% RH. However, a slight increased particle size was found when the sample was stored at 40 ± 2 °C/75 ± 5% RH storage conditions. Plausible cause might be the elevated kinetic energy imparted by temperature leading to collision and enhanced likelihood of aggregation. Furthermore, the nanosuspension did not demonstrate any indication of coalescing and caking phenomenon. Stability study indicated that the developed LP-NS showed good stability at both the storage conditions. Overall, the findings can be wrapped up by saying the lyophilized formulations are more stable when compared to the wet nanodispersion of LUF.

### 3.6.10. In vitro dissolution study

The main feature of formulating nanosuspension is to increase the solubility and dissolution rate of the poorly soluble drugs. *In vitro* drug release study is an indirect

method to evaluate the bioavailability of a formulation, where higher dissolution rate of nanosuspension possibly be due to greater surface area of nanoparticles as compared to macro-particles in pure LUF [48]. The comparative *in vitro* drug release profile of pure LUF, marketed LUF formulation, and LP-NS was presented in Figure 9(d), which represented significant variance. This change was observed due to the change in surface area with the presence of a surfactant. It showed increased drug release from LP-NS compared with pure LUF, which might be attributed to its hydrophobic nature and poor aqueous solubility [10]. Marketed dry syrup formulation showed increased drug release when compared to the pure LUF. Release of LUF from the developed LP-NS was >90% within the timeframe of initial 15 min, while those of pure LUF was only 10% which was >60% for the commercial formulation. This might be due to the several underlying reasons, such as, decreased particle size of LUF in nanosuspension results in increased surface area; an increase in the surface wetting by co-grinding with stabilizer in nanosuspension could also further increase in the dissolution; use of hydrophilic surfactant (Polysorbate 80) forms hydrophilic environment around LUF and increased wetting of the drug. Hence, increased the diffusion coefficient of drug [49]; decrease in the diffusion distance with decreased particle size lead enhancement in saturation solubility due to amorphous nature of LUF in nanosuspension [50], due to less energy requirement for breaking lattice structure in amorphous form when compared to crystalline form of the drug. Further, the particles in nanosuspension have more chances of interaction with the solvent due to small particle size that may lead to enhanced solubility [51]. Nanosuspension formulation showed approximately ~8 times increase in drug release in comparison to pure LUF which indicated that this approach can offer improved drug release characteristics. Results of this study evidently indicated that nanosuspension formulation is a successful technique to improve the dissolution rate of LUF, which is congruent to the reported reports in literature [52,53].

### 3.6.11. *In vitro* antimalarial activity

*In vitro* antimalarial activity results showed that LP-NS could be active against *P. falciparum* 3D7 strain at a very low concentration. However, the vehicle control comprising aqueous stabilizer (HPMC, PVPK30 and SLS) solution showed no activity against the tested strains. The  $IC_{50}$  value of LP-NS was found to be 0.375 ng/mL, suggesting  $IC_{50}$  value of nano-sized LUF to be 0.1 ng/mL (since amount of LUF in LUF LP-NS is 26.7% w/w). Therefore, comparing the  $IC_{50}$  value of nanosized LUF (0.1 ng/mL) (LP-NS) with pure, free form of LUF (16.0 ng/mL), marketed dry syrup formulation (4.5 ng/mL) and standard antimalarial drug chloroquine (3.5 ng/mL), it could be inferred that there was 160-fold, 45-fold and 35 fold decrease in  $IC_{50}$  value, respectively.

The enhanced *in vitro* performance of nanoformulation against the selected strains of *P. falciparum* is encouraging, which might be because of the smaller particle size and complex structure. Morphological modification of the formulation provides immense surface area that is capable to enhance the dissolution rate and consequently marked absorption.



## 4. Conclusion

Anti-solvent precipitation and ultrasonication method was employed in the present experiment to fabricate LUF nanosuspensions in order to increase the dissolution of poorly water-soluble drug. The LUF nanosuspension was successfully prepared and optimized using  $3^2$  full factorial design. Among all formulation batches, F3 showed lowest particle size and minimum  $t_{90}$  value. Optimized LUF nanosuspension was lyophilized and analyzed using DSC, XRPD and FT-IR, which indicated complex formation between LUF, soya lecithin and PVPK30. This complex converts crystalline drug in amorphous form, which might be responsible for increased solubility of drug, which was confirmed by *in vitro* release characteristics of LUF from LP-NS. Further, the antiplasmodial activity of the produced LP-NS was found to be favorable with that of the pure LUF, the marketed dry syrup formulation LUF and commercial chloroquine. Moreover, this nanosuspension could be easily administered by pediatric and geriatric population or by any person having difficulties in swallowing oral solid dosage forms, like tablets and capsules.

## Acknowledgments

Authors of the manuscript would like to thank Mangalam drugs and organics, India for providing us the gift sample of LUF. The authors of the manuscript do not have any financial conflict of interest.

## Disclosure statement

There is no conflict of interest and disclosures associated with the manuscript.

## ORCID

Prashant Kesharwani  <http://orcid.org/0000-0002-0890-769X>

## References

- [1] Norman FF, Comeche B, Chamorro S, et al. Update on the major imported protozoan infections in travelers and migrants. *Future Microbiol.* 2020;15:213–225.
- [2] Malaria. 2020. [accessed 2020 Aug 7]. Available from: <https://www.who.int/news-room/fact-sheets/detail/malaria>.
- [3] Muhindo MK, Kakuru A, Jagannathan P, et al. Early parasite clearance following artemisinin-based combination therapy among Ugandan children with uncomplicated *Plasmodium falciparum* malaria. *Malar J.* 2014;13:1–8.
- [4] Kilonzi M, Minzi O, Mutagonda R, et al. Comparison of malaria treatment outcome of generic and innovator's anti-malarial drugs containing artemether-lumefantrine combination in the management of uncomplicated malaria amongst Tanzanian children. *Malar J.* 2019;18:1–8.
- [5] Achan J, Talisuna AO, Erhart A, et al. Quinine, an old anti-malarial drug in a modern world: role in the treatment of malaria. *Malar J.* 2011;10:144.
- [6] Wahajuddin SP, Singh KSR, Raju A, et al. Intravenous pharmacokinetics, oral bioavailability, dose proportionality and in situ permeability of anti-malarial lumefantrine in rats. *Malar J.* 2011;10:293.

- [7] Lindenberg M, Kopp S, Dressman JB. Classification of orally administered drugs on the World Health Organization Model list of essential medicines according to the biopharmaceutics classification system. *Eur J Pharm Biopharm.* 2004;58(2):265–278.
- [8] Ashley EA, Stepniewska K, Lindegårdh N, et al. How much fat is necessary to optimize lumefantrine oral bioavailability? *Trop Med Int Health.* 2007;12(2):195–200.
- [9] Ezzet F, Mull R, Karbwang J. Population pharmacokinetics and therapeutic response of CGP 56697 (artemether + benflumetol) in malaria patients. *Br J Clin Pharmacol.* 1998; 46(6):553–561.
- [10] Gahoi S, Jain GK, Tripathi R, et al. Enhanced antimalarial activity of lumefantrine nanopowder prepared by wet-milling DYNO MILL technique. *Colloids Surf B Biointerfaces.* 2012;95:16–22.
- [11] Lefèvre G, Thomsen MS. Clinical pharmacokinetics of artemether and lumefantrine (Riamet®). *Clin Drug Investig.* 1999;18:467–480.
- [12] Shende P, Desai P, Gaud RS, et al. Engineering of microcomplex of artemether and lumefantrine for effective drug treatment in malaria. *Artif Cells Nanomed Biotechnol.* 2017;45(8):1597–1604.
- [13] Garg A, Bhalala K, Tomar DS. In-situ single pass intestinal permeability and pharmacokinetic study of developed lumefantrine loaded solid lipid nanoparticles. *Int J Pharm.* 2017;516:120–130.
- [14] Patel K, Sarma V, Vavia P. Design and evaluation of lumefantrine - oleic acid self nanoemulsifying ionic complex for enhanced dissolution. *DARU.* 2013;21(1):27.
- [15] Parashar D, Aditya NP, Murthy RSR. Development of artemether and lumefantrine co-loaded nanostructured lipid carriers: physicochemical characterization and *in vivo* anti-malarial activity. *Drug Deliv.* 2016;23(1):123–129.
- [16] Shakeel K, Raisuddin S, Ali S, et al. Development and *in vitro/in vivo* evaluation of artemether and lumefantrine co-loaded nanoliposomes for parenteral delivery. *J Liposome Res.* 2019;29(1):35–43.
- [17] Trasi NS, Bhujbal SV, Zemlyanov DY, et al. Physical stability and release properties of lumefantrine amorphous solid dispersion granules prepared by a simple solvent evaporation approach. *Int J Pharm.* 2020;2:100052.
- [18] Wang Y, Wang C, Zhao J, et al. A cost-effective method to prepare curcumin nanosuspensions with enhanced oral bioavailability. *J Colloid Interface Sci.* 2017;485:91–98.
- [19] Junghanns J-UAH, Müller RH. Nanocrystal technology, drug delivery and clinical applications. *Int J Nanomed.* 2008;3(3):295–309.
- [20] Li M, Azad M, Davé R, et al. Nanomilling of drugs for bioavailability enhancement: a holistic formulation-process perspective. *Pharmaceutics.* 2016;8(2):17.
- [21] Malamatarı M, Somavarapu S, Taylor KMG, et al. Solidification of nanosuspensions for the production of solid oral dosage forms and inhalable dry powders. *Expert Opin Drug Deliv.* 2016;13(3):435–450.
- [22] Verma S, Kumar S, Gokhale R, et al. Physical stability of nanosuspensions: investigation of the role of stabilizers on Ostwald ripening. *Int J Pharm.* 2011;406(1–2):145–152.
- [23] Salazar J, Ghanem A, Müller RH, et al. Nanocrystals: comparison of the size reduction effectiveness of a novel combinative method with conventional top-down approaches. *Eur J Pharm Biopharm.* 2012;81(1):82–90.
- [24] Wu L, Zhang J, Watanabe W. Physical and chemical stability of drug nanoparticles. *Adv Drug Deliv Rev.* 2011;63(6):456–469.
- [25] Al Ashmawy AZG, Eissa NG, El Nahas HM, et al. Fast disintegrating tablet of doxazosin mesylate nanosuspension: preparation and characterization. *J Drug Deliv Sci Technol.* 2020. doi: [10.1016/j.jddst.2020.102210](https://doi.org/10.1016/j.jddst.2020.102210).
- [26] Sharma C, Desai MA, Patel SR. Effect of surfactants and polymers on morphology and particle size of telmisartan in ultrasound-assisted anti-solvent crystallization. *Chem Pap.* 2019;73(7):1685–1694.

- [27] Akrawi SH, Gorain B, Nair AB, et al. Development and optimization of naringenin-loaded chitosan-coated nanoemulsion for topical therapy in wound healing. *Pharmaceutics*. 2020;12(9):893.
- [28] Mauludin R, Müller RH, Keck CM. Development of an oral rutin nanocrystal formulation. *Int J Pharm*. 2009;370(1–2):202–209.
- [29] Kumbhar SA, Kokare CR, Shrivastava B, et al. Preparation, characterization, and optimization of asenapine maleate mucoadhesive nanoemulsion using Box-Behnken design: in vitro and in vivo studies for brain targeting. *Int J Pharm*. 2020;586:119499.
- [30] Choudhury H, Gorain B, Karmakar S, et al. Improvement of cellular uptake, in vitro antitumor activity and sustained release profile with increased bioavailability from a nanoemulsion platform. *Int J Pharm*. 2014;460(1–2):131–143.
- [31] Trager W, Jensen JB. Human malaria parasites in continuous culture. *Science*. 1976;193(4254):673–675.
- [32] Fidock DA, Rosenthal PJ, Croft SL, et al. Antimalarial drug discovery: efficacy models for compound screening. *Nat Rev Drug Discov*. 2004;3(6):509–520.
- [33] Johnson JD, Denuall RA, Gerena L, et al. Assessment and continued validation of the malaria SYBR Green I-based fluorescence assay for use in malaria drug screening. *Antimicrob Agents Chemother*. 2007;51(6):1926–1933.
- [34] Kesharwani P, Banerjee S, Padhye S, et al. Parenterally administrable nano-micelles of 3, 4-difluorobenzylidene curcumin for treating pancreatic cancers. *Colloids Surf B Biointerfaces*. 2015; 132:138–145.
- [35] Dhumal RS, Biradar SV, Yamamura S, et al. Preparation of amorphous cefuroxime axetil nanoparticles by sonoprecipitation for enhancement of bioavailability. *Eur J Pharm Biopharm*. 2008;70(1):109–115.
- [36] Homayouni A, Sadeghi F, Nokhodchi A, et al. Preparation and characterization of celecoxib solid dispersions; comparison of poloxamer-188 and PVP-K30 as carriers. *Iran J Basic Med Sci*. 2014;17(5):322–331.
- [37] Loh ZH, Samanta AK, Sia Heng PW. Overview of milling techniques for improving the solubility of poorly water-soluble drugs. *Asian J Pharm Sci*. 2015;10(4):255–274.
- [38] Ribeiro A, Figueiras A, Santos D, et al. Preparation and solid-state characterization of inclusion complexes formed between miconazole and methyl-beta-cyclodextrin. *AAPS PharmSciTech*. 2008;9(4):1102–1109.
- [39] Liu D, Xu H, Tian B, et al. Fabrication of carvedilol nanosuspensions through the anti-solvent precipitation-ultrasonication method for the improvement of dissolution rate and oral bioavailability. *AAPS PharmSciTech*. 2012;13(1):295–304.
- [40] Jiang T, Han N, Zhao B, et al. Enhanced dissolution rate and oral bioavailability of simvastatin nanocrystal prepared by sonoprecipitation. *Drug Dev Ind Pharm*. 2012;38(10):1230–1239.
- [41] Phale M, Pawar S, Patil P, et al. A simple and precise method for quantitative analysis of lumefantrine by planar chromatography. *Pharm Methods*. 2010;1(1):44–48.
- [42] Patel SM, Doen T, Pikal MJ. Determination of end point of primary drying in freeze-drying process control. *AAPS PharmSciTech*. 2010;11(1):73–84.
- [43] Gitua J, Beck A, Rovers J. Quality and stability of artemether-lumefantrine stored under ambient conditions in rural Mali. *Malar J*. 2014;13: 474.
- [44] Wlodarski K, Sawicki W, Paluch KJ, et al. The influence of amorphization methods on the apparent solubility and dissolution rate of tadalafil. *Eur J Pharm Sci*. 2014;62:132–140.
- [45] Cheow WS, Kiew TY, Yang Y, et al. Amorphization strategy affects the stability and supersaturation profile of amorphous drug nanoparticles. *Mol Pharm*. 2014;11(5):1611–1620.
- [46] Lindfors L, Forssén S, Skantze P, et al. Amorphous drug nanosuspensions. 2. Experimental determination of bulk monomer concentrations. *Langmuir*. 2006;22(3):911–916.

- [47] Gommes CJ. Ostwald ripening of confined nanoparticles: chemomechanical coupling in nanopores. *Nanoscale*. 2019;11(15):7386–7393.
- [48] Patel VR, Agrawal YK. Nanosuspension: an approach to enhance solubility of drugs. *J Adv Pharm Technol Res*. 2011;2(2):81–87.
- [49] Lindfors L, Skantze P, Skantze U, et al. Amorphous drug nanosuspensions. 1. Inhibition of Ostwald ripening. *Langmuir*. 2006;22(3):906–910.
- [50] Wang Y, Zheng Y, Zhang L, et al. Stability of nanosuspensions in drug delivery. *J Control Release*. 2013;172(3):1126–1141.
- [51] Jacob S, Nair AB, Shah J. Emerging role of nanosuspensions in drug delivery systems. *Biomater Res*. 2020;24:3.
- [52] Kathpalia H, Salunkhe S, Juvekar S. Formulation of gastroretentive sustained release floating in situ gelling drug delivery system of solubility enhanced curcumin-soy lecithin complex. *J. Drug Deliv Sci Technol*. 2019;53:101205.
- [53] Sajeev Kumar B, Saraswathi R, Venkates Kumar K, et al. Development and characterization of lecithin stabilized glibenclamide nanocrystals for enhanced solubility and drug delivery. *Drug Deliv*. 2014;21(3):173–184.